Radial X-Ray Diffraction Study of Static Strength of Tantalum to 80 GPa *

Lun Xiong(熊伦)[1,2,3**], Li-Gang Bai(白利刚)[3], Xiao-Dong Li(李晓东)[3], Jing Liu(刘景)[3]

[1]*School of Intelligent Manufacturing, Sichuan University of Arts and Science, Dazhou 635000*
[2]*Dazhou Industrial Technology Institute of Intelligent Manufacturing, Dazhou 635000*
[3]*Beijing Synchrotron Radiation Facility, Institute of High Energy Physics, Chinese Academy of Sciences, Beijing 100049*

(Received 21 June 2017)

We study the strength and texture of tantalum (Ta) under uniaxial compression up to 80 GPa using an angle-dispersive radial x-ray diffraction technique together with the lattice strain theory in a diamond anvil cell at ambient temperature. The ratio of differential stress to shear modulus (t/G) is found to remain constant above ∼60 GPa, indicating that the Ta starts to experience macro yield with plastic deformation at this pressure. Combined with independent constraints on the high-pressure shear modulus, we find that the Ta sample could support a differential stress of ∼4.67 GPa when it starts to yield with plastic deformation at ∼60 GPa under uniaxial compression. The differential stress in Ta ranges from 0.216 GPa to 4.67 GPa with pressure increasing from 1 GPa to 60 GPa and can be expressed as $t = 0.199(33) + 0.075(1)P$, where P is the pressure in GPa. A maximum differential stress as high as ∼5.37 GPa can be supported by Ta at the high pressure of ∼80 GPa. In addition, we investigate the texture of Ta under nonhydrostatic compression to 80 GPa using the software package material analysis using diffraction. It is proven that the plastic deformation due to stress under high pressures is responsible for the development of texture.

PACS: 61.05.cp, 62.20.F−, 07.35.+k, 64.30.Ef DOI: 10.1088/0256-307X/34/10/106101

Equation of state of Ta has generated considerable interest in previous experimental studies.[1−11] Featherston *et al.*[1−5] have investigated the compression behavior of Ta under high pressure using ultrasound and obtained the bulk modulus ranging from 190 GPa to 195 GPa. Wang *et al.*[6] obtained the bulk modulus as 195.24 GPa with shock compression. Tang *et al.*[7] derived the zero-pressure bulk modulus $K_0 = 192.65(3.08)$ GPa with its pressure derivate $K_0' = 3.58(0.11)$ from high-pressure x-ray diffraction (XRD) data. Errandonea *et al.*[8] performed the high-pressure XRD and obtained $K_0 = 190(15)$ GPa with $K_0' = 3.7(0.5)$. Guinan *et al.*[9] reported a zero-pressure bulk modulus K_0 of 193 GPa with its pressure derivation of 3.15 from high-pressure XRD in a diamond anvil cell (DAC). Cynn *et al.*[10] measured the compressional behavior of Ta and obtained a bulk modulus $K_0 = 194.7(7.8)$ GPa with $K_0' = 3.4(0.1)$ fitting the data at high pressures. Dewaele *et al.*[11] performed the high-pressure XRD of Ta and obtained $K_0 = 198(3.4)$ GPa with $K_0' = 3.07(0.14)$. In the experimental studies on compressibility of Ta, the previous results[1−11] present tiny discrepancies of EoS parameters and slight relative errors.

In addition, the yield strength of Ta has been investigated in the static compression[12] and shock compression.[13] Dewaele and Loubeyre[12] have studied the yield strength of Ta single crystals to 93 GPa in a DAC. Within the experimental error, they obtained a yield strength as high as 4.4 GPa at the pressure of 93 GPa. Subsequently, Asay *et al.*[13] investigated the yield strength of Ta under shock compression to 18 GPa, and they obtained a yield strength of 1.6 GPa at the elastic limit.

Despite many experiments for its equation of state,[1−11] there are only two direct experimental measurements for its strength.[12,13] Moreover, it is interesting to note the large loss of yield strength in Ta under shock compression[12] compared with static XRD performed by Asay *et al.*[13] In this study, we investigated the Ta sample under nonhydrostatic compression using the angle dispersive XRD technique in a radial DAC (rDAC). Together with the lattice strain theory[14,15] as well as the calculated high-pressure shear modulus, the strength and texture of Ta up to a confining pressure of 80 GPa are obtained.

A two-fold paranomic DAC with a pair of beveled diamond anvils (300-μm culet diameter) was used to exert uniaxial compression on the Ta sample in the radial x-ray diffraction (RXRD) measurements. A beryllium gasket was pre-indented to ∼25-μm thickness at ∼20 GPa and drilled a 60-μm-diameter hole in the center of pre-indentation as the sample chamber. Special attention was paid to make sure that the sample hole was well centered with respect to the anvil culet. Powder Ta sample (<2 μm, with a purity of 99.9% from Alfa Aesar) was loaded into the gasket hole and a ruby chip with diameter of ∼10 μm was placed on top of the sample center serving as a pressure marker.[16] The choice for the pressure standard of ruby[16] was motivated as it has no overlapping lines added to the diffraction pattern of the Ta sample and is well-calibrated at high pressures. No pressure-transmitting medium was used to ensure maximum

*Supported by the National Natural Science Foundation of China under Grant Nos 10875142 and 11079040, and the Chinese Academy of Sciences under Grant Nos KJCX2-SW-N03 and KJCX2-SW-N20.
**Corresponding author. Email: 1094129778@qq.com
© 2017 Chinese Physical Society and IOP Publishing Ltd

nonhydrostatic stresses. By design, the DAC was tilted to an angle of 28° to minimize the contribution of Be diffraction lines to the sample patterns.[17]

Angle-dispersive RXRD experiments were performed at 4W2 beam line of Beijing Synchrotron Radiation Facility (BSRF), Chinese Academy of Sciences (CAS). A Si(111) monochromator was used to tune the synchrotron source with a wavelength of 0.6199 Å, and the incident monochromatic x-ray beam was focused by a pair of Kirkpatrick–Baez mirrors to approximately 30(vertical) × 8(horizontal) of full width at half maximum (FWHM) spot and directed through the Be gasket and the sample. The two-dimensional diffraction patterns were collected by a Mar345 image plate detector (pixel size 100×100 μm^2) and the two-dimensional diffraction rings on the image plate were integrated with the program Fit2D[18] to obtain one-dimensional intensity curve of the diffraction patterns as a function of the 2θ angel. The distance and orientation of the detector were calibrated using a CeO_2 standard. At each increasing pressure, the RXD pattern was collected typically for 15–20 min after about 30 min to allow for stress relaxation.

The RXRD data was analyzed using the lattice strain theory[14,15] developed by Singh and Balasingh. According to the lattice strain theory,[14,15] the measured d-spacing $d_{\rm m}(hkl)$ is a function of the azimuthal angle ψ between the DAC loading axis and the diffraction plane normal (hkl), and can be calculated using the relation as

$$d_{\rm m}(hkl) = d_{\rm p}(hkl)[1 + (1 - 3\cos^2\psi)Q(hkl)], \quad (1)$$

where $d_{\rm m}(hkl)$ is the measured d spacing, and $d_{\rm p}(hkl)$ is the d spacing under equivalent hydrostatic pressure, and $Q(hkl)$ is the orientation-dependent lattice strain.

Under isostress conditions (the Reuss limit), the differential stress t can be expressed as

$$t = 6G\langle Q(hkl)\rangle, \quad (2)$$

where $\langle Q(hkl)\rangle$ represents the averaged value of Q over all observed reflections, and G is the aggregate shear modulus of the sample. The pressure dependence of G can be obtained from extrapolation of ultrasonic or theoretically calculated single-crystal elasticity constant. If the differential stress t has reached its limiting value of yield strength at high pressures when materials start to deform plastically, $6\langle Q(hkl)\rangle = t/G$ will reflect the ratio of yield strength to shear modulus. In addition, this ratio may be a good qualitative indicator of hardness as it reflects the contributions of both plastic and elastic deformation.[19]

Equation (1) indicates that $d_{\rm m}(hkl)$ versus $(1 - 3\cos^2\psi)$ exhibits a straight line, and $d_{\rm m}(hkl)$ reaches the maximum at $\psi = 90°$ and the minimum at $\psi = 0°$. At $\psi = 54.7°(1-3\cos^2\psi = 0)$, the positions of the observed XRD lines reflect the d spacing due to the mean component of stress, thus the equivalent hydrostatic compression curve can be directly derived from the diffraction data at $\psi = 54.7°$. The slope of $d_{\rm m}(hkl)$ versus $1-3\cos^2\psi$ relation products $d_{\rm p}(hkl)Q(hkl)$ directly related to the ratio of differential to shear modulus $(t/G = 6\langle Q(hkl)\rangle)$ and $d_{\rm p}(hkl)$ can be directly measured at $\psi = 54.7°$. Combined with independent constraints on the high-pressure shear modulus, the differential stress or yield strength at high pressure can be determined.

In a conventional angle-dispersive RXRD experiment, the incident x-ray beam is perpendicular to the compression axis and passes through a Be gasket and the Be gasket would contribute intense diffraction lines to the sample patterns. Thus we can tilt the DAC to an α angle to minimize the contribution of Be diffraction lines to the sample patterns.[17] In this geometry, ψ corresponding to the angle between the diffracting plane normal and the loading axis is calculated by[20]

$$\cos\psi_{hkl} = \sin\alpha\cos\delta\cos\theta_{hkl} + \cos\alpha\sin\theta_{hkl}, \quad (3)$$

where θ is the diffraction angle, and δ is the azimuthal angle in the plane of the detector.

The RXRD diffraction patterns are integrated over each azimuthal sector with 5° internal plots of x-ray intensity as a function of two-theta to fit peak positions, intensities, and FWHM of the diffraction peaks. To determine the variation of the diffraction peaks' positions with δ, we use this software package to integrate the diffraction patterns and fit peak positions with segments of 5° intervals in the azimuth angle, in the range of 90°–180°. RXRD spectra of Ta are collected up to an equivalent pressure of 80 GPa, where pressures are derived from the ruby chip.[16]

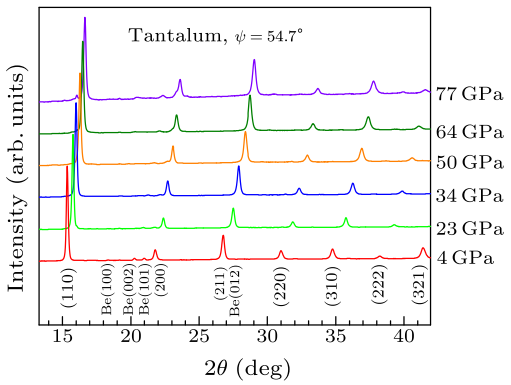

Fig. 1. Selected diffraction patterns of Ta under nonhydrostatic compression taken at $\psi = 54.7°$. The pressures are determined from the ruby marker.

Figure 1 shows the selected 2θ-intensity diffraction patterns of the sample taken at $\psi_{hkl} = 54.7°$ under different pressures. Seven diffraction peaks of bcc phase in Ta (110, 200, 211, 220, 310, 222, 321) are observed at 4 GPa. Diffraction peak positions are fitted with pseudo-Voigt line shapes using the software package Multifit 4.2.

The variation of $d_{\rm m}(hkl)$ with $1-3\cos^2\psi$ for Ta (110), (211), (220) and (310) diffraction lines at six selected pressures is shown in Fig. 2. As expected from the theory,[14,15] the measured d-spacings vary linearly with $1-3\cos^2\psi$.

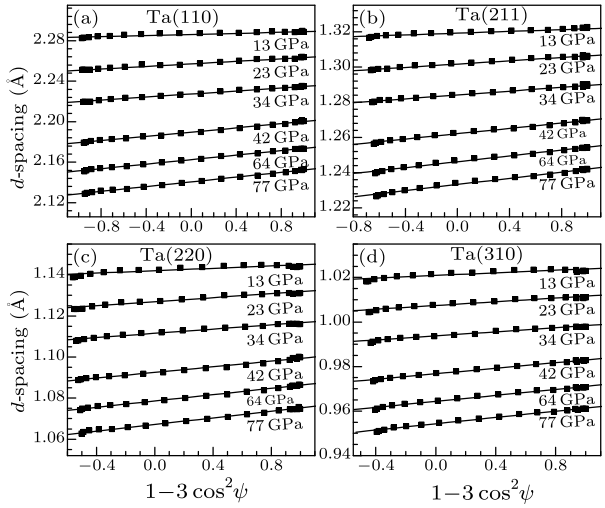

Fig. 2. Dependence of observed d-spacing on $1-3\cos^2\psi$ for Ta (110), (211), (220) and (310) diffraction lines at six selected pressures. The solid lines are least-square fits to the data.

For angle-dispersive RXRD experiments, the d-spacings of $d_{\rm p}(110)$, $d_{\rm p}(200)$, $d_{\rm p}(211)$, $d_{\rm p}(220)$ and $d_{\rm p}(310)$ determined at $(1-3\cos^2\psi)=0$ ($\psi=54.7^\circ$) were used to least-squares fitting to calculate the lattice parameter a of Ta. The pressure dependence of the normalized lattice parameters of the bcc phase is shown in Fig. 3. The fitting result of entire pressure range yields

$$\frac{a}{a_0}=1-1.64\times10^{-3}P+7.41\times10^{-6}P^2. \quad (4)$$

The relative change along the axis is about 8.46% from 1 GPa to 80 GPa. In addition, the compression behavior of a shows a good regularity in the entire pressure range in this work.

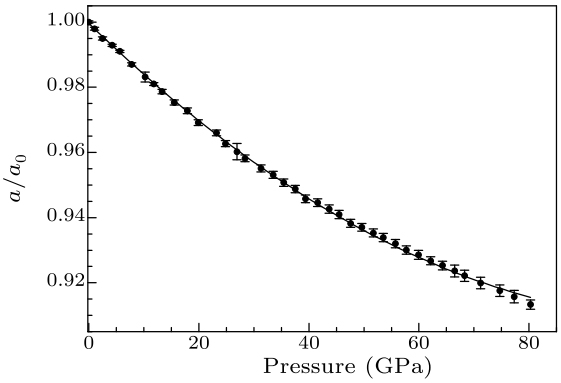

Fig. 3. Compressibility of the normalized lattice parameter of Ta. The solid line is polynomial fitting line to the data.

According to Eq. (1), the orientation-dependent lattice strain $Q(hkl)$ can be derived from the slope of the linear relationship between the observed d spacing and $1-3\cos^2\psi=0$. The ratio of t/G is obtained from the average value of $Q(hkl)$ over all observed reflections. Figure 4 shows that the ratio of differential stress to shear modulus ($t/G=6\langle Q(hkl)\rangle$) as a function of pressure for Ta. The ratio of t/G is found to remain constant above ~60 GPa, indicating that the Ta sample starts to suffer macro yield with plastic deformation at ~60 GPa and t/G reaches its limiting value of 0.036 at this pressure. As well as γ-Si_3N_4,[21] there is no sharp transition of Ta from Fig. 4. We think that the mechanism for this especial phenomenon may be due to its high hardness and high shear strength.

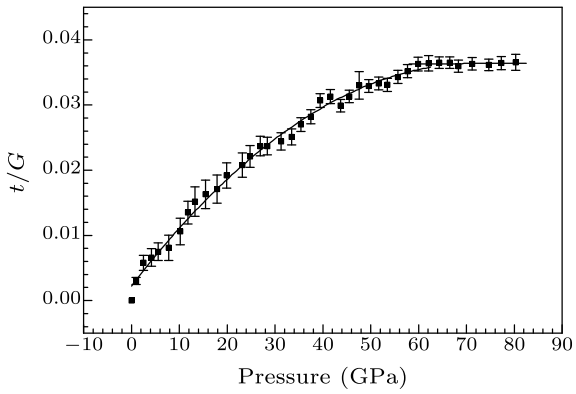

Fig. 4. Ratio of differential stress to shear modulus (t/G) as a function of pressure for Ta. The pressures of Ta are determined from the ruby sensor. The estimated errors are obtained from the scatter of $d(hkl)$ versus $1-3\cos^2\psi$.

With the high-pressure shear modulus known, the differential stress can be derived at each pressure step from $t=6G\langle Q(hkl)\rangle$. The volume-dependent shear modulus G of the polycrystalline aggregate is given by[22]

$$G=G_0(1+2f)^{5/2}\Big[1+(3K_0\frac{dG_0}{dP}\frac{1}{G_0}-5)f\Big], \quad (5)$$

where $f=[(V_0/V)^{2/3}-1]$, B_0 and G_0 are the bulk modulus and shear modulus at ambient pressure, respectively. Using the single-crystal elastic modulus,[23] the values of G of Ta at high pressures are derived from Eq. (5) as a function of V_0/V.

Figure 5 compares differential stresses of Ta together with differential stress obtained by Dewaele *et al.*[12] and the RXRD results.[24–27] It can be seen that the differential stress t increases more slowly above ~60 GPa, indicating that the Ta starts to suffer macro yield at ~60 GPa with plastic deformation and t reaches its limiting value of 4.67 GPa at this pressure. The differential stress of Ta fitted to the linear fit to the data from 1 GPa to 60 GPa changes continuously with increasing pressure and yields $t=0.199(33)+0.075(1)P$, where P is the pressure in GPa. However, the yield strength fitted to the linear fit to the data from 62 GPa to 80 GPa yields $t=$

$2.694(106) + 0.033(2)P$ (GPa). A maximum differential stress t as high as ∼5.37 GPa can be supported by Ta at the high pressure of 80 GPa. In addition, the differential stress of present work is slightly higher than the differential stress obtained from Dewaele *et al.*[12] and much higher than the yield strength of 1.6 GPa obtained by Asay *et al.*[13] The differences may be due to different starting Ta samples, experimental methods, and/or hydrostaticity, as Mao *et al.*[28] and Chijioke *et al.*[29] pointed out that the strength differences between static data and shock compression could be a significant source of error in DAC experiments when the pressure is not hydrostatic. In addition, shock compression leads to high temperatures which hinders the increase of the uniaxial stress.[30] It can be seen that the strength of Ta is much higher than those of Au[25,26] and Nb;[27] while the differential stress sustained by Ta is less than those of Mo[27] and W,[24] and much less than that of Re.[26]

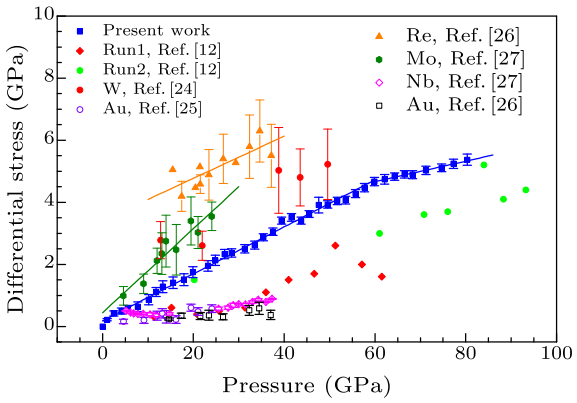

Fig. 5. Differential stress as a function of pressure for Ta compared with the data obtained by Dewaele *et al.*[12] and other radial x-ray diffraction results.[24–27] The solid squares are determined from this work. The solid diamonds are the differential stress for run 1 obtained from x-ray diffraction of Ref. [12]. The solid circles are the differential stress for run 2 obtained from x-ray diffraction of Ref. [12]. For differential stress, the error bars reflect the experimental error and the uncertainties in shear modulus at high pressure.

Recently, Hu *et al.*[31] reported a kink of longitudinal sound velocities of Ta as a function of shock pressure at 60 GPa, while the bulk sound velocities show no discontinuity. They explained that the observed longitudinal sound velocity discontinuity may result from structural transformation or an electronic topological transition. Accordingly, this interpretation is very consistent with the conclusion drawn by Burakovsky *et al.*[32] and Hsiung *et al.*[33] Burakovsky *et al.*[32] predicted a phase transition of Ta at ∼70 GPa using first-principle calculations. Subsequently, Hsiung *et al.*[33] found a possible phase transition of Ta from shock compression at 45 GPa using transmission electron microscopy. They ascribed the mechanism transition to reasons that the high shock pressure suppresses the dynamic-recovery reaction and leads to shear transformation of Ta. Interestingly, the plastic deformation of Ta happens at ∼60 GPa due to the shear stress in the present work. The pressure of ∼60 GPa obtained from the present work and Hu *et al.*[31] is higher than 45 GPa obtained by Hsiung *et al.*,[33] as the shear stress between shock compression and static compression in the DAC is quite different and the shock compression leads to high temperatures, which blocks the increase of the uniaxial stress.[30]

The plastic deformation by dislocation glide results in crystallite rotations, generating lattice-preferred orientation (LPO) or texture if the material deforms by slip or mechanical twinning, and intensity variations along the Debye rings are indicative of preferred orientation (texture) due to plastic deformation. In radial x-ray diffraction geometry, texture is revealed by variation of intensity along the Debye rings obtained by Mar345 image plate and we can extract quantitative texture information using the software package material analysis using diffraction (MAUD).[34,35] Figure 6 compares inverse pole figures for Ta to 77 GPa. At low pressures, the strong (111) and (011) texture of Ta is consistent with the typical bcc metals attributed to dominant $110\langle -111\rangle$ slip.[36] However, after 60 GPa when plastic deformation happens, the (001) lattice plane is the most profound LPO which is also more compressible than other planes with increasing the pressure. It is proven that this texture is developed by the plastic deformation due to stress under high pressures, as individual crystals deform preferentially on slip planes when the shear stress is applied to polycrystals.[37] In addition, at higher pressures, the (111) lattice plane becomes more compressible again.

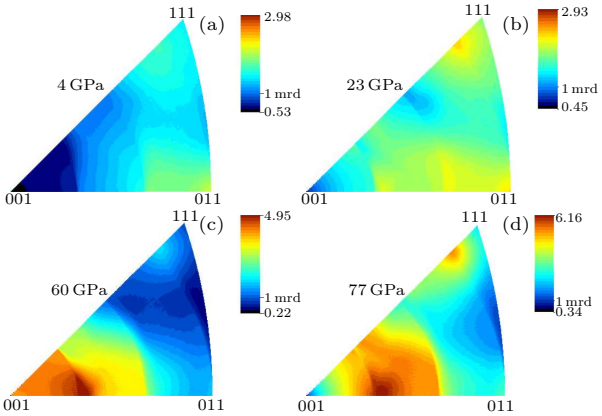

Fig. 6. Inverse pole figures of Ta along the compression direction (normal direction) at high pressures. Texture strength is expressed as *mrd*, where $mrd = 1$ denotes random distribution, and a higher *mrd* value represents stronger texture. The figures are derived from the RXRD patterns evaluated using the MAUD program.

In summary, we have determined the strength and texture of Ta up to 80 GPa in a DAC under non-hydrostatic compression using the RXRD technique at ambient temperature. The ratio of t/G increases more slowly above ∼60 GPa indicating that Ta experiences macro yield with plastic deformation. Together

with estimates of the high-pressure shear modulus, we find that the Ta sample could support a differential stress of ∼4.67 GPa when it starts to yield with plastic deformation at ∼60 GPa under uniaxial compression. A maximum differential stress t as high as ∼5.37 GPa can be supported by Ta at the high pressure of ∼80 GPa. In addition, texture of Ta under nonhydrostatic compression up to the highest pressure has been investigated using the software package MAUD. It is proven that the plastic deformation due to stress under high pressures is responsible for the development of texture.

References

[1] Featherston F H and Neighbours J R 1963 *Phys. Rev.* **130** 1324
[2] Soga N 1966 *J. Appl. Phys.* **37** 3416
[3] Leisure R G, Hsu D K and Seiber B A 1973 *J. Appl. Phys.* **44** 3394
[4] Katahara K W, Manghnani M H and Fisher E S 1976 *J. Appl. Phys.* **47** 434
[5] Sarrao J L, Chen S R, Visscher W M, Lei M, Kocks U F and Migliori A 1994 *Rev. Sci. Instrum.* **65** 2139
[6] Wang Y, Ahuja R and Johansson B 2002 *J. Appl. Phys.* **92** 6616
[7] Tang L Y, Liu L, Liu J, Xiao W S, Li Y C, Li X D and Bi Y 2010 *Chin. Phys. Lett.* **27** 016402
[8] Errandonea D, Somayazulu M, Hausermann D and Mao H K 2003 *J. Phys.: Condens. Matter* **15** 7635
[9] Guinan M W and Steinberg D J 1974 *J. Phys. Chem. Solids* **35** 1501
[10] Cynn H and Yoo C S 1999 *Phys. Rev.* B **59** 8526
[11] Dewaele A, Loubeyre P and Mezouar M 2004 *Phys. Rev.* B **69** 092106
[12] Dewaele A and Loubeyre P 2005 *Phys. Rev.* B **72** 134106
[13] Asay J R, Ao T, Vogler T J, Davis J P and Gray III G T 2009 *J. Appl. Phys.* **106** 073515
[14] Singh A K 1993 *J. Appl. Phys.* **73** 4278
[15] Singh A K and Balasingh C 1994 *J. Appl. Phys.* **75** 4956
[16] Mao H K, Xu J and Bell P M 1986 *J. Geophys. Res.* **91** 4673
[17] Xiong L, Liu J, Bai L G, Li Y C, Lin C L, He D W, Peng F and Lin J F 2013 *J. Appl. Phys.* **113** 033507
[18] Hammersley A P, Svensson S O, Hanfland M, Fitch A N and Hausermann D 1996 *High Press. Res.* **14** 235
[19] Duffy T S, Elert M, Furnish M D, Chau R, Holmes N and Nguyen J 2007 *AIP Conference Proceedings* **135** 639
[20] Merkel S, Wenk H R, Shu J F, Shen G Y, Gillet P, Mao H K and Hemley R J 2002 *J. Geophys. Res.* **107** ECV 3-1
[21] Kiefer B, Shieh S R, Duffy T S and Sekine T 2005 *Phys. Rev.* B **72** 014102
[22] Singh A K, Jain A, Liermann H P and Saxena S K 2006 *J. Phys. Chem. Solids* **67** 2197
[23] Katahara K W, Manghnani M H and Fisher E S 1979 *J. Phys.* F **9** 773
[24] He D W and Duffy T S 2006 *Phys. Rev.* B **73** 134106
[25] Duffy T S, Shen G Y, Shu J F, Mao H K, Hemley R J and Singh A K 1999 *J. Appl. Phys.* **86** 6729
[26] Duffy T S, Shen G Y, Heinz D L, Shu J F, Ma Y Z, Mao H K, Hemley R J and Singh A K 1999 *Phys. Rev.* B **60** 15063
[27] Singh A K and Liermann H P 2011 *J. Appl. Phys.* **109** 113539
[28] Mao H K, Bell P M, Shaner J W and Steinberg D J 1978 *J. Appl. Phys.* **49** 3276
[29] Akobuije A D, Nellis W J and Silvera I F 2005 *J. Appl. Phys.* **98** 073526
[30] Jeanloz R and Godwal B K 2012 *J. Phys.: Conf. Ser.* **377** 012032
[31] Hu J B, Dai C D, Yu Y Y, Liu Z J, Tan Y, Zhou X M, Tan H, Cai L C and Wu Q 2012 *J. Appl. Phys.* **111** 033511
[32] Burakovsky L, Chen S P, Preston D L, Belonoshko A B, Rosengren A, Mikhaylushkin A S, Simak S I and Moriarty J A 2010 *Phys. Rev. Lett.* **104** 255702
[33] Hsiung L M and Lassila D H 2000 *Acta Mater.* **48** 4851
[34] Lutterotti L, Matthies S and Wenk H R 1999 *Proceeding of the Twelfth International Conference on Textures of Materials (ICOTOM-12)* **1** 1599
[35] Lutterotti L, Matthies S and Wenk H R 1999 *MAUD: a friendly Java program for material analysis using diffraction* p 14
[36] Rollett A D and Texture S I 2000 *Anisotropy Preferred Orientations in Polyscrystals, Their Effect on Materials Properties* 2nd edn (Cambridge: Cambridge University Press) chapter 5 p 178
[37] Chen B, Lutker K, Raju S V, Yan J Y, Kanitpanyacharoen W, Lei J L, Yang S Z, Wenk H R, Mao H K and Williams 2012 *Science* **338** 1448